Irrigation is a considerable nitrogen input in global cropland

J Serra[1,2,3]; L Lassaletta[4]; G Ros[5]; M Quemada[4]; F Giannini-Kurina[1]; E Aguilera[6]; M Graversgaard[1]; C Marques-dos-Santos[3]; MR Cameira[7]; W De Vries[5]; A Dobermann[8]; X Zhang[9]; J Rahimi[2,10]; T Dalgaard[1,2]; K Butterbach-Bahl[2,10]

[1] Department of Agroecology, Aarhus University, Blichers Allé 20, 8830, Tjele, Denmark

[2] Center for Landscape Research in Sustainable Agricultural Futures (Land-CRAFT), Aarhus University, Ny Munkegade 114, DK-8000, Aarhus C, Denmark

[3] Forest Research Centre, Associate Laboratory TERRA, School of Agriculture, University of Lisbon, 1349-017, Lisbon, Portugal

[4] CEIGRAM/ETSIAAB, Universidad Politécnica de Madrid, 28040, Madrid, Spain

[5] Environmental Systems Analysis Group, Wageningen University and Research, Wageningen, the Netherlands

[6] Instituto de Economía, Geografía y Demografía, Consejo Superior de Investigaciones Científicas, Madrid, Spain

[7] LEAF-Linking Landscape, Environment, Agriculture and Food-Research Center, Associated Laboratory TERRA, Instituto Superior de Agronomia, Universidade de Lisboa, Tapada da Ajuda, 1349-017, Lisbon, Portugal

[8] International Fertiliser Association (IFA) Paris France

[9] Appalachian Laboratory, University of Maryland Center for Environmental Science, 301 Braddock Road, Frostburg, MD 21532, USA

[10] Institute of Meteorology and Climate Research, Atmospheric Environmental Research (IMK-IFU), Karlsruhe Institute of Technology (KIT), Garmisch-Partenkirchen, Germany

Supplementary Material

Table of Contents

Supplementary methods

Crop names in the empirical data

Vegetables – vegetables (not specified), spinach, cauliflower, eggplant, pepper, casaba, cucumber, onion, garlic, melon, lettuce, broccoli, endive

Other crops – amaranth, sunflower, cantaloupe, sugar beet, poppy, oats, rapeseed, alfalfa, others/NA (crop not specified), flowers, tomato

Spatially explicit cropland N inputs 2010-2019

Harvested areas, yield and production

We used harvested areas and production for the year 2020 from MapSPAM as the basemaps. We scaled the basemaps according to FAOSTAT country totals to produce annual average maps for the period 2010-2019. Yields were computed as the ratio of production and harvested areas.

Cropland nitrogen inputs

We computed gridded cropland nitrogen inputs for the period 2010-2019 at 100 km^2 as the sum of synthetic fertilisers, manure, atmospheric deposition and biological fixation. Synthetic fertilisers, manure and deposition were derived from [1]. Atmospheric deposition was adjusted according to the share of cropland in a 100 km^2 grid. For symbiotic biological fixation, we employed the methodology developed[2] for grain legumes, including soybean and groundnut. This work synthesized published data to develop crop-specific coefficients and/or empirical relationships. These enable the estimation of crop-specific N_2 fixation based on crop production. We separated symbiotic nitrogen fixation from grain legumes from non-symbiotic nitrogen fixation from rice and sugarcane. We did this by subtracting the total biological nitrogen fixed by rice and sugarcane, assuming a non-symbiotic nitrogen fixing rate of 25 kg N ha^{-1} yr^{-1} per FAOSTAT.

Upscaling with machine learning

Spatial predictors

All the spatial predictors used are identified in Table S1. We would like to highlight specifically differences that may arise from observed and gridded irrigation and nitrogen inputs since these were, by far, the most important predictors. Firstly, we were unable to retrieve information from the different studies concerning specific irrigation efficiencies, even when irrigation systems were reported. This contrasts with the spatially explicit crop irrigation which do not account for different irrigation systems. A similar issue occurs with nitrogen inputs: whereas in the field observations these concern inputs of irrigated- and crop-specific systems, the gridded data focus on total cropland nitrogen inputs as no better data exists currently.

Machine learning framework

We hyper-tuned a random forests model using different cross-validation strategies given the highly clustered observational dataset. We tested eight different sampling strategies. Firstly, we tested a typical 70/30 partition (70% training, 30% testing) stratified by site and a random 10-fold cross-validation with five repetitions. Secondly, we tested different leave-one-out cross validation according to different variables: site, a k-means cluster (based on covariates), first level administrative boundaries (GADM) and pedoclimatic clusters based on Koppen-Geiger climate zones and USDA soil texture. Lastly, we employed a 5- and 10-fold nearest neighbour distance matching leave-one-out cross validation[3].

Although, in theory, the best performances were achieved by a 70/30 partition and the random 10-fold cross validation (Fig. S10), we opted to disregard it since it tends to inflate performance metrics in clustered datasets[4]. More importantly, we preferred to maximise predictive domain (i.e., area of applicability) to generalise the model as much as possible. This was not achieved through both the 70/30 partition and 10-fold cross validation where observations from the same study were present in training and testing folds/partitions. This not only creates a data bias in the hyper-tuned model but also limits the spatial coverage when training the model, inflating performance. The former because it did not include all the crops within all the regions, so therefore the “high” performance was artificially and not well represented by regions nor crops. A similar situation occurred with the latter, which trained and validated the predictions using observations from the region, artificially inflating the model’s performance. This also greatly reduced the area of applicability of the model.

It is important to note the impact of the different cross-validation strategies in our multi-scaled estimates of N_{Irrig}. Therefore, we also compared the predictions at different spatial scales (Fig. S13-14).

Supplementary results

Plausibility assessment of the estimated nitrogen input from irrigation

To evaluate the plausibility of our global N_{Irrig} estimates and to understand their sensitivity to key assumptions, we applied two complementary methods. While these do not constitute a formal validation—owing to the absence of global monitoring data—they provide important constraints on magnitude and internal consistency.

1. Inferred nitrate concentrations

We first calculated the nitrate concentration implied by our N_{Irrig} estimates by dividing the predicted total N_{Irrig} by irrigation water volume, yielding an average concentration of nitrate in irrigation water sources (including both surface- and groundwater). Across global irrigated areas, this approach resulted in a median concentration of 41 mg L^{-1} (interquartile range: 26–78 mg L^{-1}). Almost 1.5% of grid cells showed values exceeding 750 mg L^{-1}, primarily in Russia (Fig. S22), which may reflect artefacts or hotspots not fully captured by monitoring networks, and we deem these concentrations implausible.

While this approach offers a useful diagnostic, it relies on several simplifying assumptions. Most notably, it assumes that irrigation water volumes are known and that a single, blended nitrate concentration characterises each cell, regardless of source. In reality, nitrate concentrations can vary considerably between and within surface and groundwater sources, and water mixing is neither spatially uniform nor necessarily proportional to water volume. These limitations introduce uncertainty that is not captured in the median estimate, and they may suppress heterogeneity or dilute extreme values.

Further, comparisons to regional case studies illustrate both strengths and limitations of the approach. For example, the Guadalquivir basin in Spain is widely recognized as a nitrate hotspot, particularly in groundwater (>50 mg L^{-1})[5]. However, our estimates for irrigation water nitrate concentrations in the region range between 10 and 25 mg L^{-1} across much of the basin. This divergence likely reflects the fact that only 30–45% of the irrigated area is equipped for groundwater use[6], with the remainder drawing from lower-nitrate surface waters—highlighting the importance of irrigation source mix, which cannot be precisely resolved at the grid scale. A similar dynamic may be present in eastern China, where groundwater accounts for less than half of irrigated supply[6], helping to explain the relatively modest predicted concentrations in an otherwise intensively managed region[7]. Conversely, in Denmark—where all irrigation draws on groundwater—the predicted nitrate concentrations appear to be overestimated[5]. However, in the absence of spatially resolved nitrate concentrations at the irrigation source level, a rigorous quantitative comparison was not possible.

2. Exploring variability using a factorial design focussed on nitrate concentrations

To better constrain potential N_{Irrig} values under varying assumptions, we conducted a factorial analysis. For each grid cell, we combined irrigation volumes[8] and the estimated proportion of area equipped for groundwater[5] with a range of plausible nitrate concentrations. Recognising that nitrate concentrations in surface water tend to be lower than in groundwater[8], we constrained concentration ranges to 0.1–25 mg L^{-1} for surface water and 0.1–100 mg L^{-1} for groundwater. We applied uniform concentrations at the grid level and aggregated resulting N_{Irrig} values globally.

This approach does not represent actual spatial variability in nitrate concentrations, but it provides insight into the bounds of plausible N_{Irrig} estimates under varying input assumptions. Across the factorial design, global N_{Irrig} estimates varied substantially (Fig. S23), with higher values emerging in scenarios with widespread groundwater use and elevated concentrations. These results reinforce that assumptions about nitrate concentrations—particularly in groundwater—exert strong control over national and global N_{Irrig} estimates.

Limitations of current validation approaches

Despite their utility, both approaches are constrained by important structural and data limitations. Most critically:

(i) No global nitrate monitoring dataset currently exists at sufficient resolution or consistency to evaluate N_{Irrig} predictions at scale. Available datasets are fragmented, temporally sparse, or reflect only certain water bodies or monitoring networks.

(ii) Grid-scale aggregation of water volumes and land areas masks heterogeneity in both water sources and nitrate concentrations. To illustrate this, we replicated a simplified aggregation analysis using data from a European-scale study[8]. This study estimated an average irrigation water use at 53 $km^3\ yr^{-1}$, with nitrate concentrations of 16.4 mg L^{-1} (groundwater) and 1.9 mg L^{-1} (surface water). Using our mass-balance approach, we calculated a corresponding averaged N_{Irrig} of 71 Gg N yr^{-1}, which is only one-third of the study's bottom-up average of 240 Gg N yr^{-1}. We found a similar situation also in a bottom-up study from Portugal[9]: averaged values for irrigation were 2 $km^3\ yr^{-1}$ and 21 and 5 mg L^{-1} for ground- and surface water, respectively, yielding a N_{Irrig} estimate of 4.8 Gg N yr^{-1}, almost half of the averaged value. These discrepancies reflect the non-linear effects of spatial aggregation, which tend to reduce the influence of extreme values and obscure local hotspots.

Comparison of estimated nitrogen input from irrigation

A limited number of studies has focussed on the regional and national contribution of N_{Irrig} (Table S2), particularly using data-driven approaches.

Therefore, we are unable to provide meaningful comparisons with other studies in most cases. From the 11 studies we found, 5 are nitrogen budgets focussed on China. All these used fixed nitrogen irrigation rates based on Chinese literature, both in time and space, which we were unable to verify. This is a considerable limitation given the spatial and temporal variation of irrigation and nitrate dynamics, but a reasonable assumption given the scope of the studies. This, however, raises a typical problem within the scientific community of using values from other studies without plausible contexts. This is greatly exemplified by [10], where the authors assessed regional and global nitrogen flows using information for Burkina Faso[11]. Assuming global values based on a study focussed on a single country is not only an invalid assumption, but also the authors[11] derived those values from an even older work.

Some works[8,9,12] used data-driven approaches to estimate the nitrogen contribution of irrigation water. For these studies we can provide a more robust comparison, even though no validation nor calibration against observations was provided.

Comparison with [8] for the year 2010 showed significantly strong correlation coefficients ($r>0.54$), except for rice and potatoes (Fig. S6). These showed the largest differences, on a country basis, against our predictions. For rice, Italy showed the largest disparity, while for potatoes these occurred in Northern Europe (e.g., Germany, Denmark, the Netherlands).

Comparison with [13] for the year 2015 also showed a significantly strong correlation coefficient (Fig. S7) of 0.84. The largest disagreement occurred in China, where we predict 4.2 Tg N yr^{-1} and the reported value was 1.3 Tg N yr^{-1}. We are unable to provide a plausibility check for possible methodological differences for this difference, as no information about how the authors derived estimates of N_{Irrig} were provided [13].

Supplementary tables

Table S1. Comparison of our estimates with other studies according to study area (catchment, regions, countries, continents and global), and overview of the underlying methodologies used.

Study area	Estimate	Our study (2010-2019)	Description
National values for China [14]	Maize: 3.4 kg N ha^{-1} yr^{-1} Rice: 22 kg N ha^{-1} yr^{-1} Wheat: 8.1 kg N ha^{-1} yr^{-1}	*Observations (avg ± sd)* Maize: 33.9 ± 43.6 kg N ha^{-1} yr^{-1} Rice: 12.1 ± 14.8 kg N ha^{-1} yr^{-1} Wheat: 33.8 ± 29.5 kg N ha^{-1} yr^{-1} *Predicted (avg ± sd)* Maize:68.0 ± 53.7 kg N ha^{-1} yr^{-1} Rice:65.9 ± 47.5 kg N ha^{-1} yr^{-1} Wheat: 69.5 ± 57.2 kg N ha^{-1} yr^{-1}	Fixed nitrogen irrigation rates with unclear nitrate concentrations in irrigation water. Sourced from a Chinese PhD thesis.
Haihe Basin, China[15] for 2010	136 Gg N yr^{-1}	223 Gg N yr^{-1} (90 Gg N yr^{-1} assuming a fixed rate of 16 kg N ha^{-1} yr^{-1})	Fixed nitrogen irrigation rate of 16 kg N ha^{-1} yr^{-1} based on other sources for rice (3.3-25.7 kg N ha^{-1} yr^{-1}) and upland crops (2.5-28.7 kg N ha^{-1} yr^{-1})
China [16] for 2010s	0.82 Tg N yr^{-1}	4.1 Tg N yr^{-1}	Assumed coefficients from Wang et al. (2014)
China [17] for 2010	1.1 Tg N yr^{-1} (arable farms)	4.1 Tg N yr^{-1} (1.5 Tg N yr^{-1} assuming a fixed rate of 20.7 kg N ha^{-1} yr^{-1})	Fixed nitrogen irrigation rate of 20.7 kg N ha^{-1} yr^{-1} sourced from elsewhere
Global and regional flows for 2000 [10]	World: 3.3 Tg N yr^{-1} Asia: 2.1 Tg N yr^{-1} Europe: 0.32 Tg N yr^{-1} Africa: 0.29 Tg N yr^{-1} North America: 0.46 Tg N yr^{-1} South America: 0.14 Tg N yr^{-1} Oceania: 0.03 Tg N yr^{-1}	World: 14 Tg N yr^{-1} Asia: 11.1 Tg N yr^{-1} Europe: 0.33 Tg N yr^{-1} Africa: 0.76 Tg N yr^{-1} North America: 0.85 Tg N yr^{-1} South America: 0.72 Tg N yr^{-1} Oceania: 0.07 Tg N yr^{-1}	**Sum of sedimentation (from erosion) and irrigation**. Fixed nitrogen irrigation rate of 3.3×10^{-3} kg N m^{-3} based on [11], which was based on an irrigation rate of 300 mm yr^{-1} and 3.3 mg N L^{-1}.
Global [18] for the 1990s	4 (3-5) Tg N yr^{-1}	14 Tg N yr^{-1}	Fixed irrigation rate of 900-1000 mm yr^{-1} and nitrogen concentrations of 1-2 mg N kg^{-1}.
California [19]	41 Gg N yr^{-1}	53 Gg N yr^{-1}	Unclear how these estimates were derived.
US states and national for 2015 [12]	California: 29 Gg N yr^{-1} US: 154 Gg N yr^{-1}	California: 53 Gg N yr^{-1} US: 798 Gg N yr^{-1}	Based on reported crop irrigation usage per state from surface- and groundwater, with the average nitrogen concentrations accordingly.
Japan for 2010-2015[20]	44 Gg N yr^{-1}	134 Gg N yr^{-1}	Derived using sum of irrigation water from surface- and groundwater and the average total nitrogen concentration in irrigation water sources.
Regional, national and continental flows in Europe for 2010 [8]	Europe: 256 Gg N yr^{-1}	Europe: 336 Gg N yr^{-1}	Crop irrigation input estimated using a water balance model. Nitrate concentrations based on machine learning for groundwater and weighted average for surface waters.
National and global scales circa 2015 [13]	World: 8.9 Tg N yr^{-1}	World: 14 Tg N yr^{-1}	Unclear how these estimates were derived.

Table S2. Spatial predictors used in the machine learning upscaling procedure. All the final predictors were resampled to a spatial resolution of 100km2.

Type	Variable	Source	Spatial resolution
Management/ Human intervention	Crop irrigation rates 2010-2019	[21]	10 km
	Cropland nitrogen inputs 2010-2019	-	10 km
	Population density 2020	WorldPop	100 m
	Gross domestic product per capita	[22]	10 km
Groundwater	Groundwater table depth	[23]	30 arcsec
	Groundwater recharge	[24]	Polygon
	Nitrate transport velocity	[25]	10 km
	Aquifer permeability	[26]	Polygon
	Aquifer porosity		Polygon
Surface water	Distance to water	[27]	30 arcsec
	Global river flow accumulation	Hydrobasins	5 arcsec
Soil	Plant-available soil water holding capacity 1m	ISRIC	250 m
	Plant-available soil water holding capacity 2m		
	Lithology	OpenLandMap	250 m
	Landforms		250 m
	Soil organic carbon (%)		250 m
	Aridity index	[28]	30 arcsec
	Historical growing degree days	GAEZ	10 km
Climate	Maximum temperature of warmest month	Worldclim	30 arcsec
	Mean Diurnal Range		
	Mean temperature of coldest quarter		
	Mean temperature of driest quarter		
	Mean temperature of warmest quarter		
	Mean temperature of wettest quarter		
	Minimum temperature of coldest month		
	Precipitation of coldest quarter		
	Precipitation of driest month		
	Precipitation of driest quarter		
	Precipitation of warmest quarter		
	Precipitation of wettest quarter		
	Precipitation seasonality		
	Temperature seasonality		

Supplementary figures

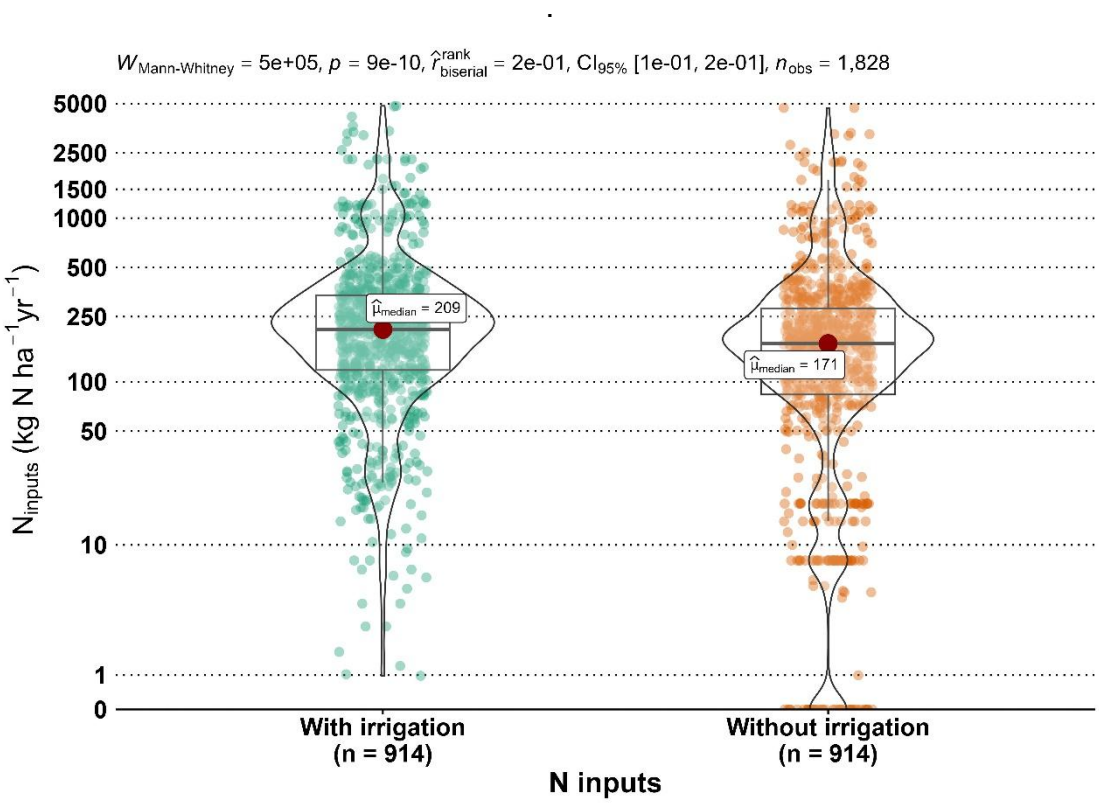

Figure S1. Pairwise comparison of (a) nitrogen inputs observations with and without irrigation.

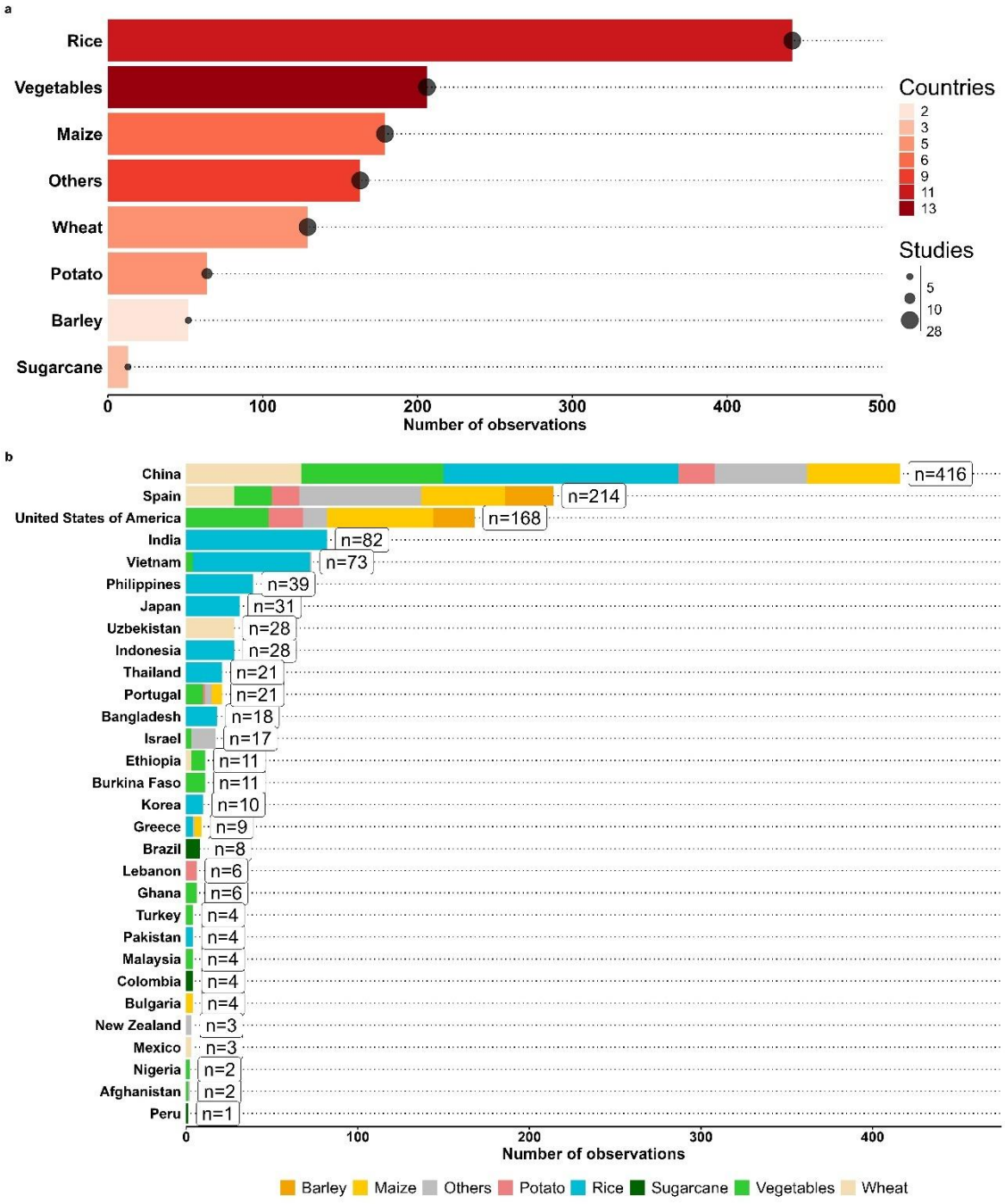

Figure S2. (a) Number of observations for each crop per number of countries and studies. (b) Number of observations for each country per crop.

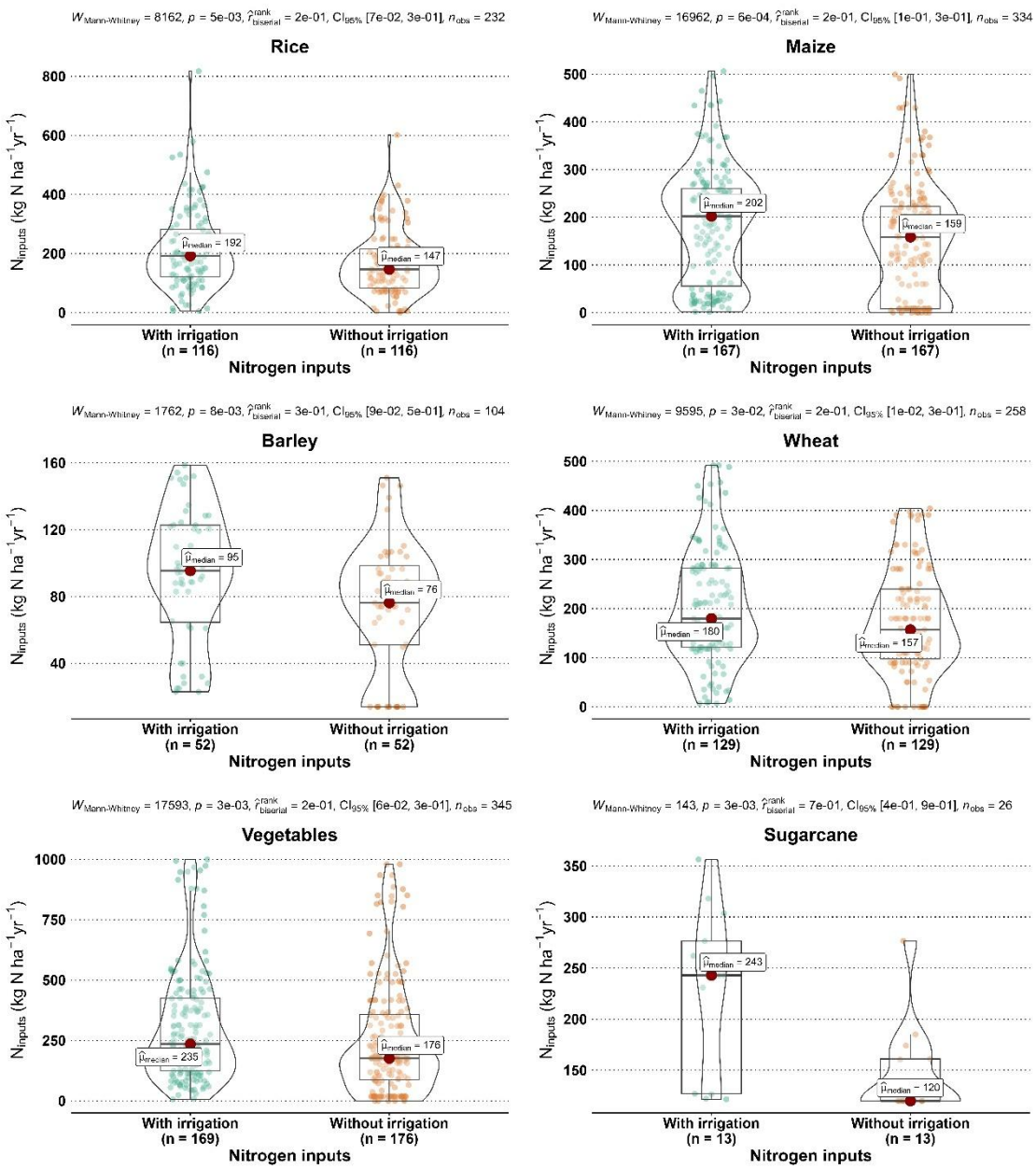

Figure S3. Comparison of observed total nitrogen inputs with and without irrigation for different crops.

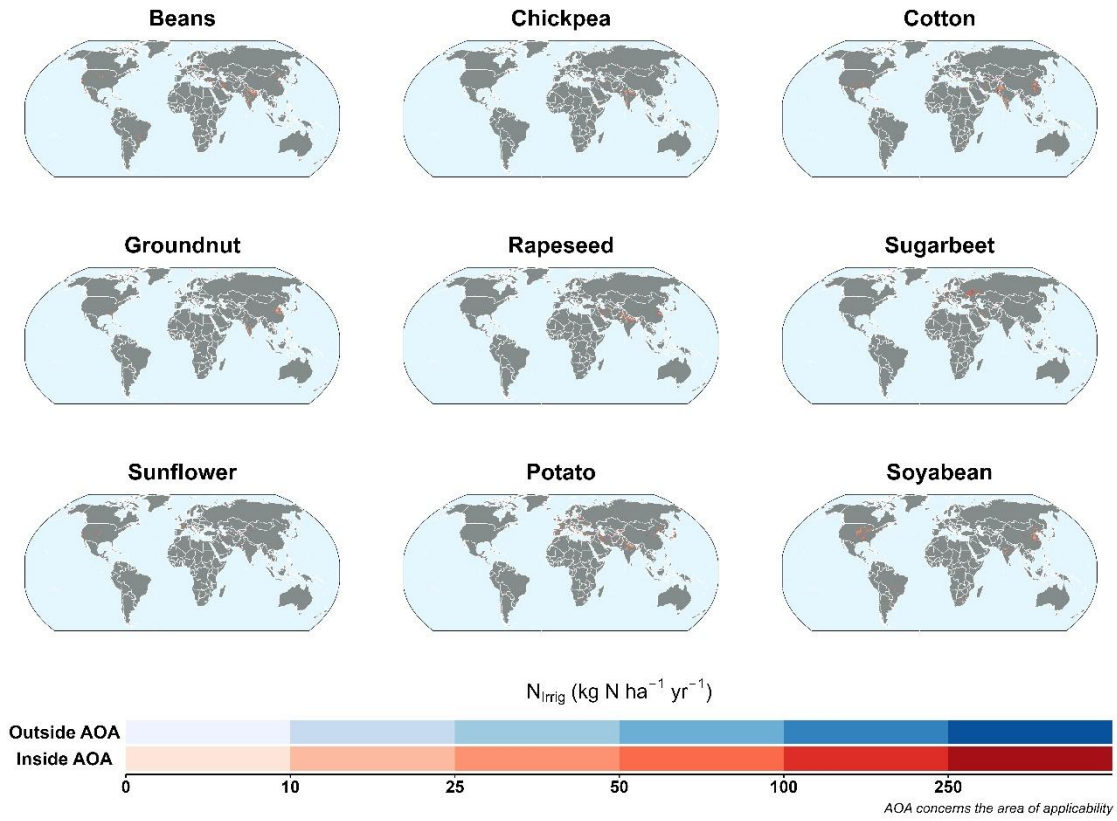

Figure S*4*. Spatial variation of the gridded predictions for "other crops for the period 2010-2019

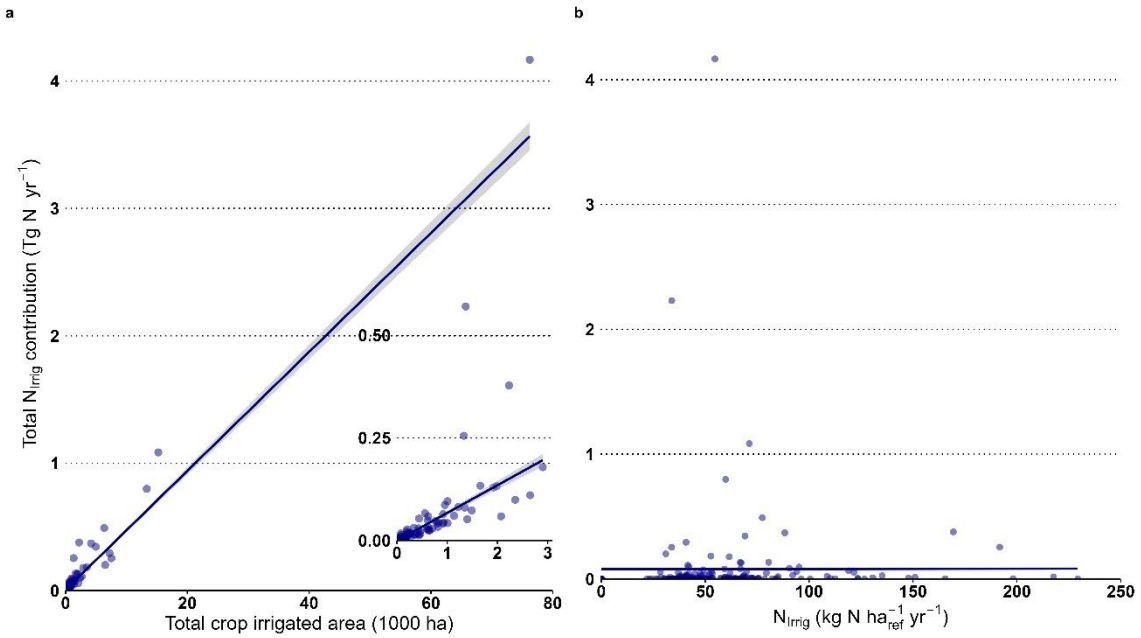

Figure S*5*. Correspondence of N_{Irrig} with total crop irrigated areas (a) and N_{Irrig} scaled by reference area at the country scale (i.e., scaled according to total crop irrigated areas). In (a) the R^2 is 0.94 ($p<0.001$) while in (b) the R^2 is around 0 ($p=0.91$).

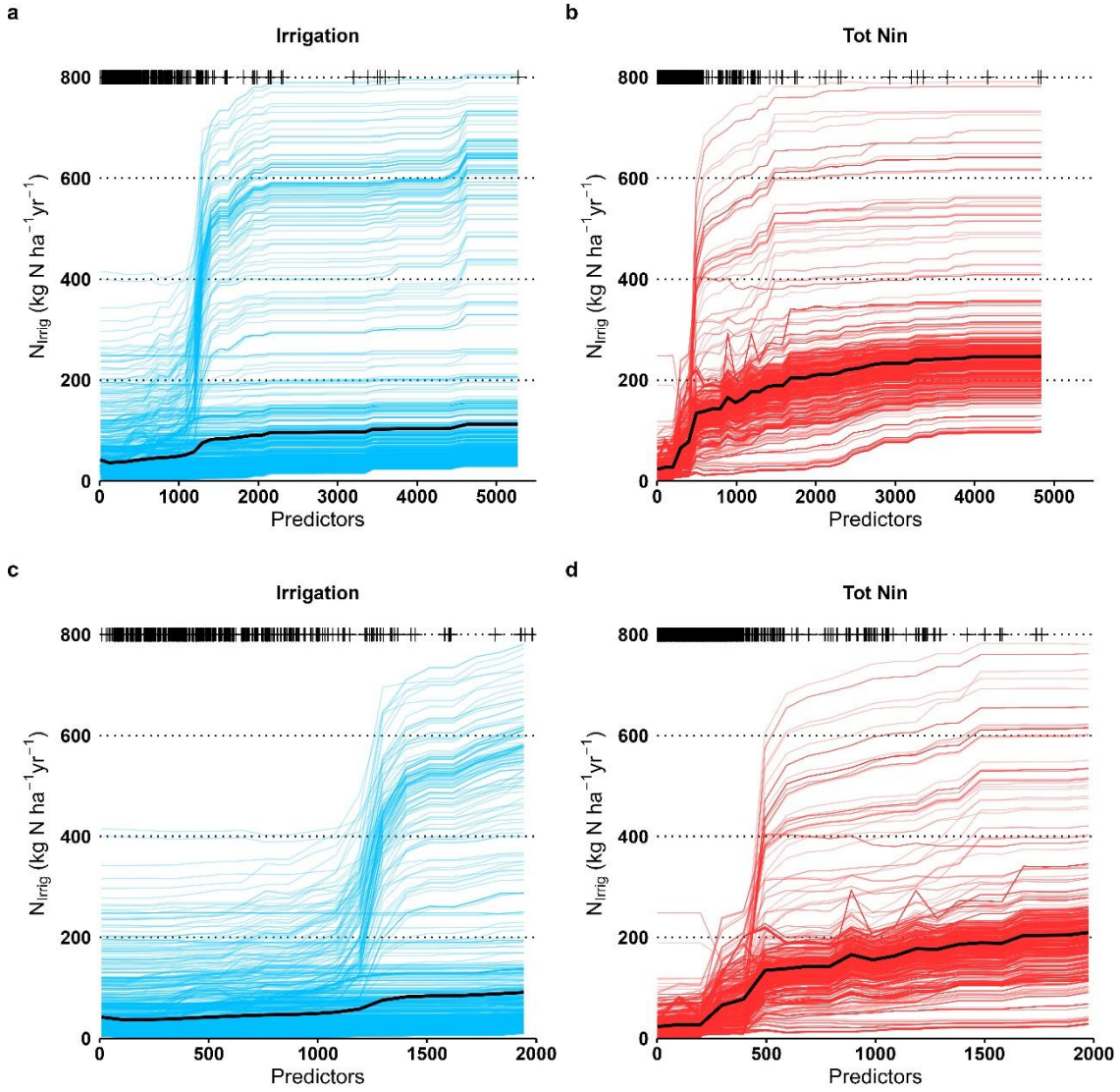

Figure S*6*. Partial dependence plot for all observations for irrigation (a) (mm yr^{-1}) and (b) total nitrogen inputs (kg N ha^{-1} yr^{-1}) with N_{Irrig} for all observations. Black lines represent the average response between the predictors and N_{Irrig}. (c) and (d) concern the partial dependence plots for irrigation and total nitrogen inputs, respectively, constrained according to the 95th percentile. Black vertical lines represent observations values for the predictors.

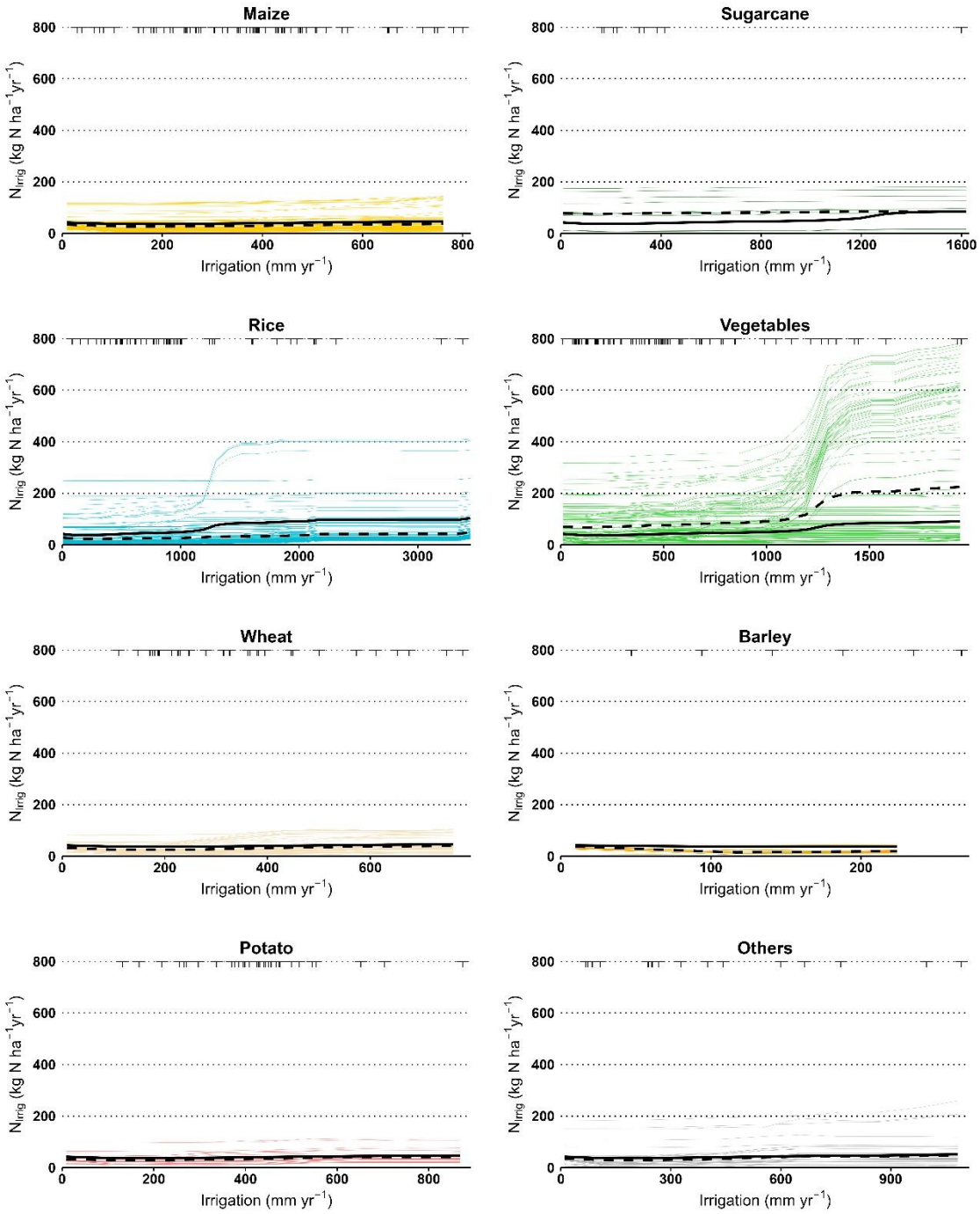

Figure S7. Partial dependence plot between irrigation rates and N_{Irrig} for different crops based on the cross-validated observational dataset. Black lines represent the overall average, while dashed lines represent the average for a given crop. Black vertical lines represent observations values for the predictors.

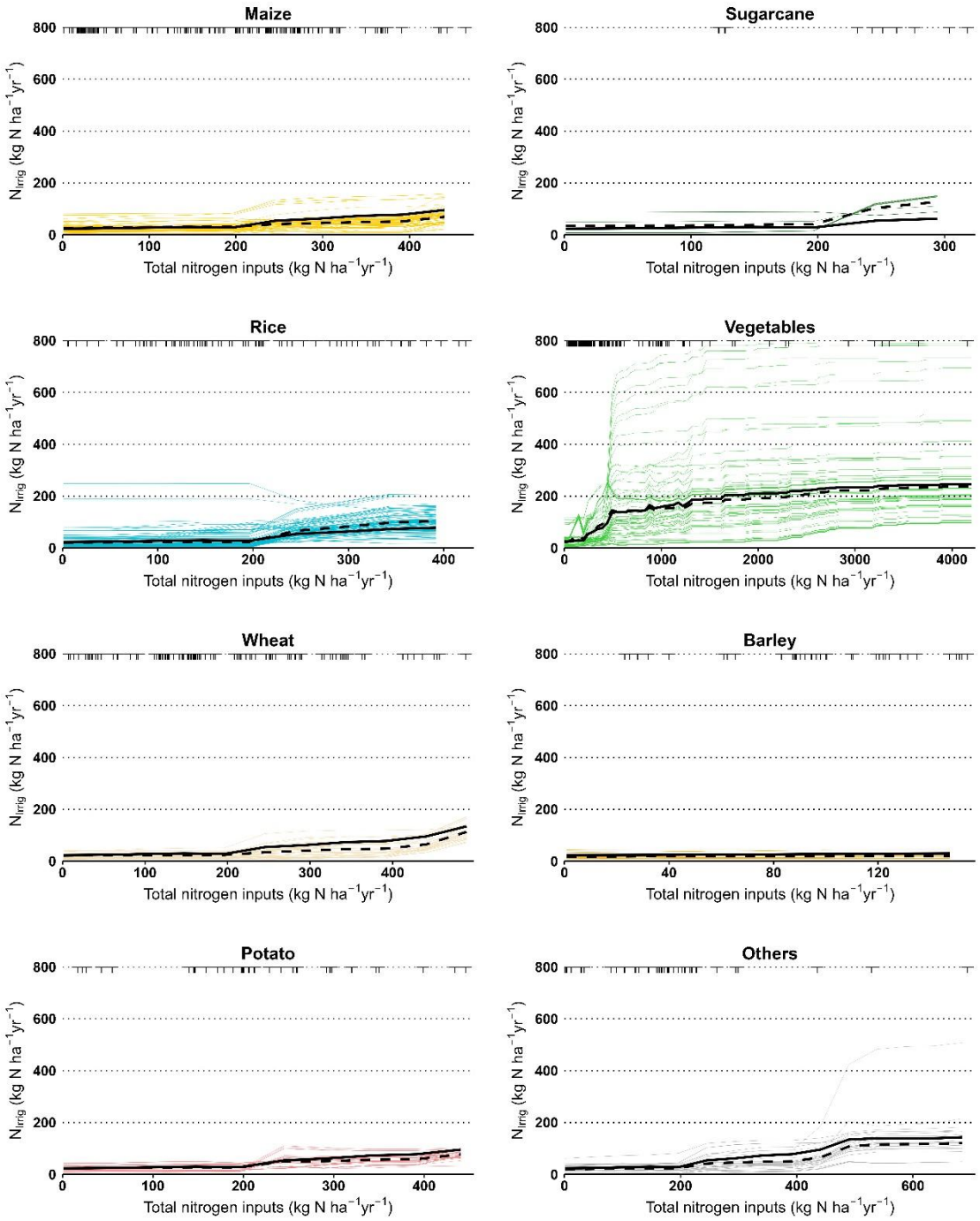

Figure S*8*. Partial dependence plot between total nitrogen inputs and N_{Irrig} for different crops based on the cross-validated observational dataset. Black lines represent the overall average, while dashed lines represent the average for a given crop. Black vertical lines represent observations values for the predictors.

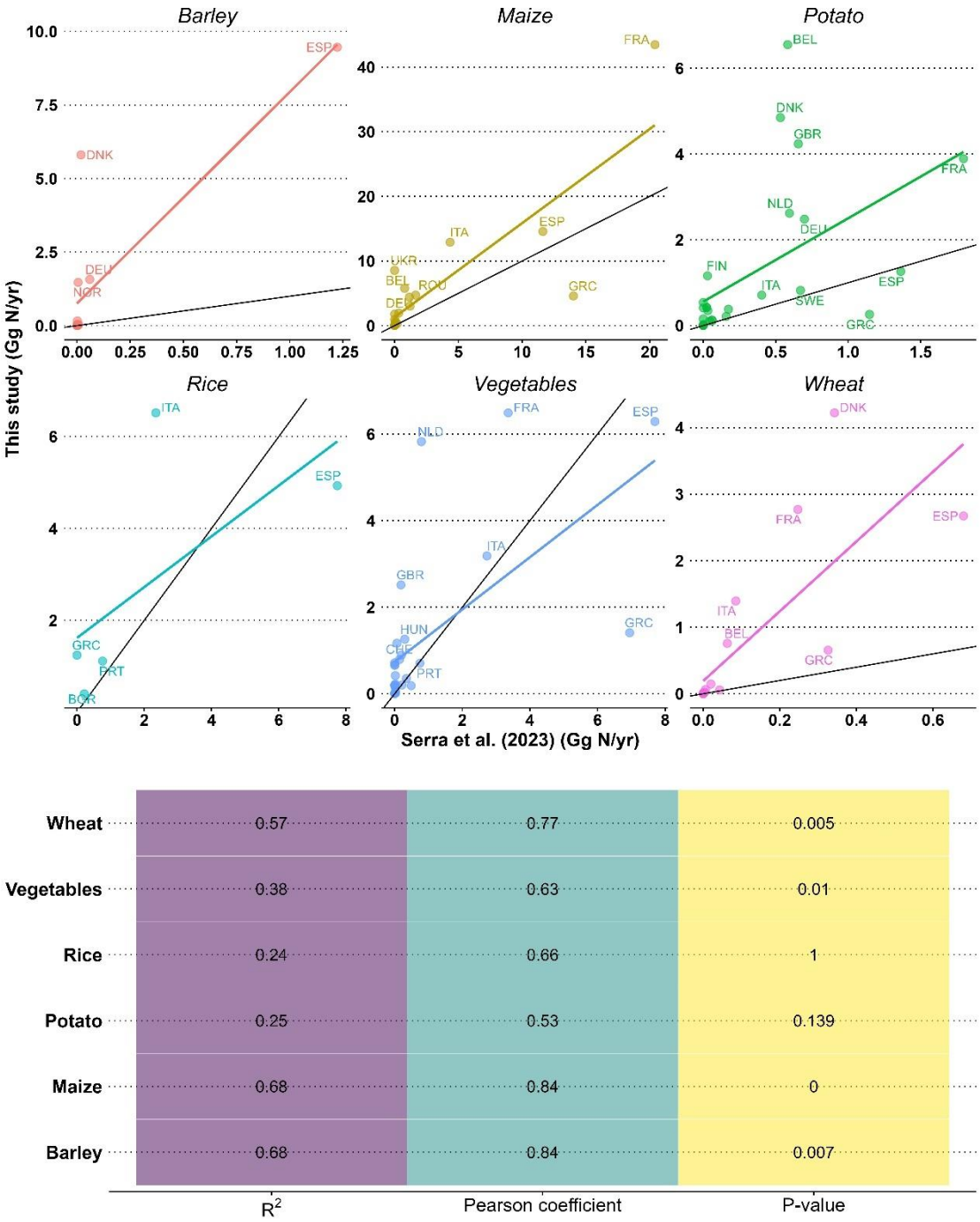

Figure S9. Scatterplot of gridded data aggregated at the country scale between this study and [8] for Europe for the year 2010, and performance metrics. Black line represents the 1:1 line. P-value was corrected using the holm method.

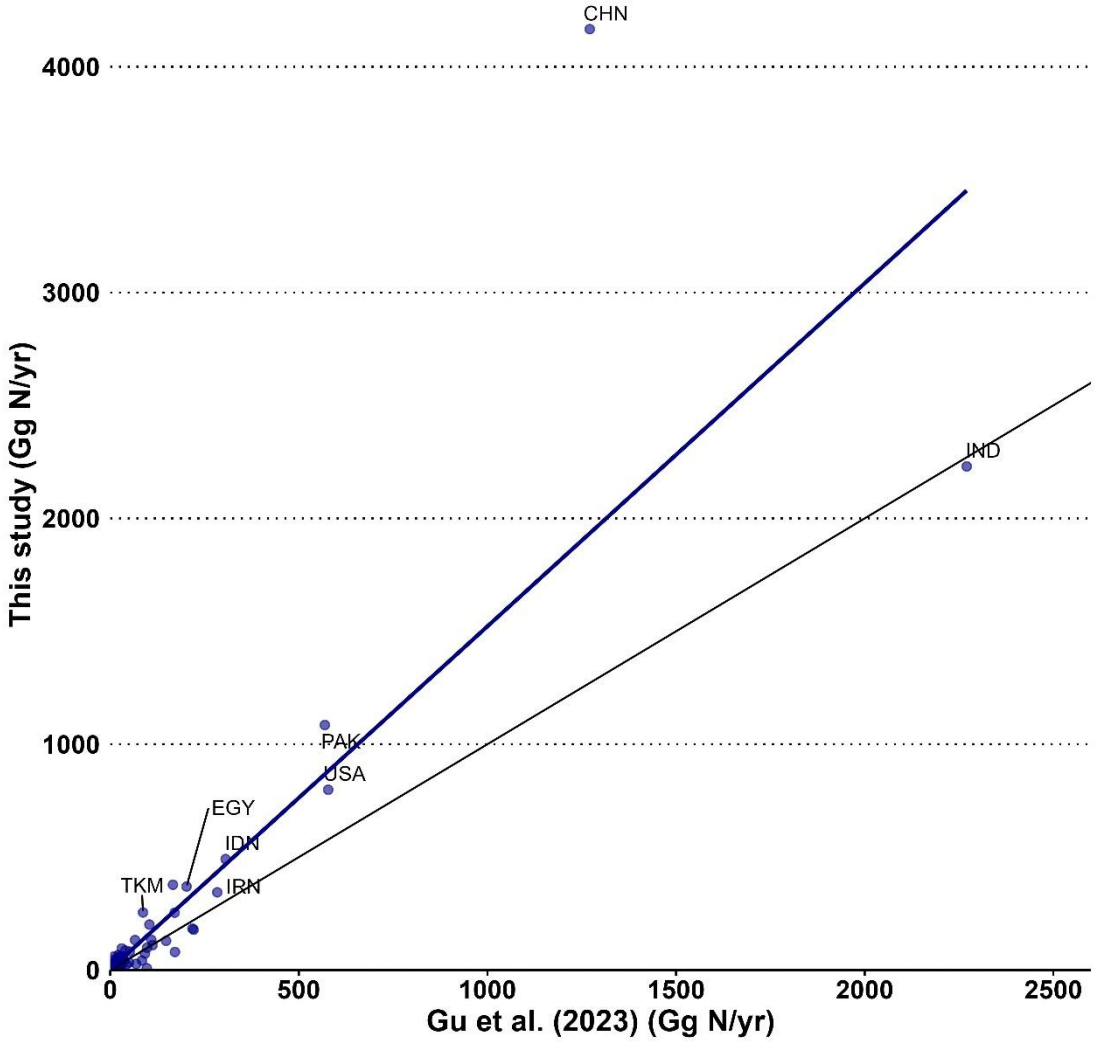

Figure S10. Scatterplot of data at the country scale between this study and [13] for the year 2015. Black line represents the 1:1 line. R^2 was 0.72 with a Pearson correlation coefficient of 0.85 ($p \approx 0$).

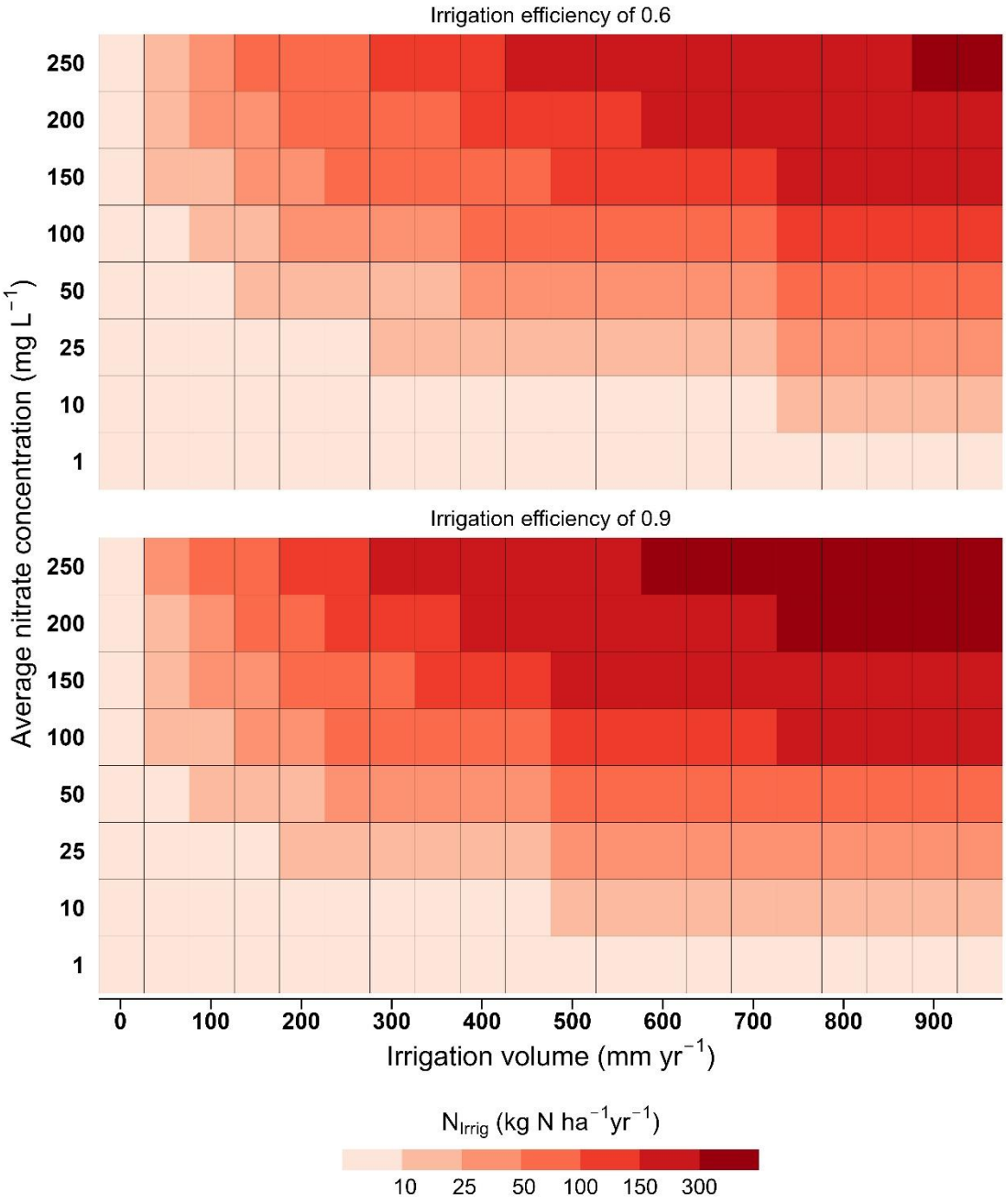

Figure S11. Contribution of the nitrogen input via irrigation water according to nitrate concentration in irrigation water sources and irrigation volume per two different irrigation efficiencies. This is calculated as mandated in the Portuguese Nitrate Vulnerable Zones (https://www.dgadr.gov.pt/diretiva-nitratos/codigo-boas-praticas-agricolas): N_{Irrig} = 0.000226 x nitrate x (irrigation x 10) x efficiency. Note that for lower irrigation efficiencies N_{Irrig} is lower, but the nitrate losses through leaching/runoff will, in principle, be comparatively higher.

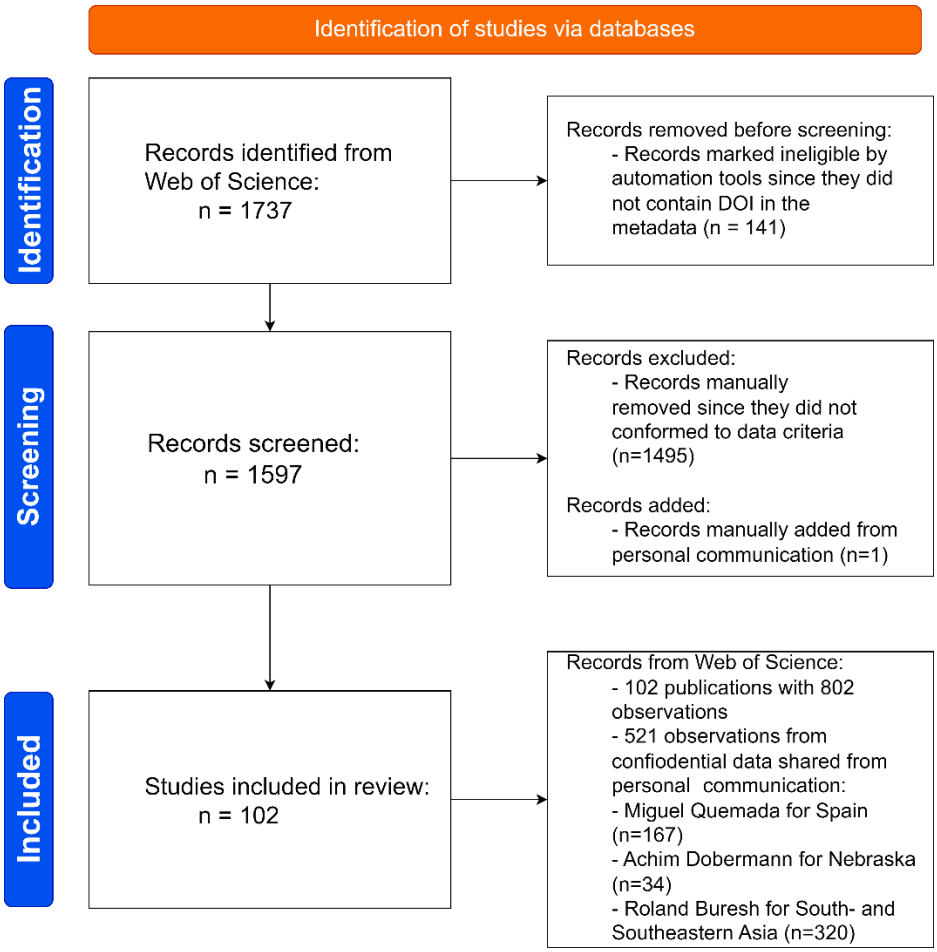

Figure S12. PRISMA guidelines for the synthesis of the global field observations.

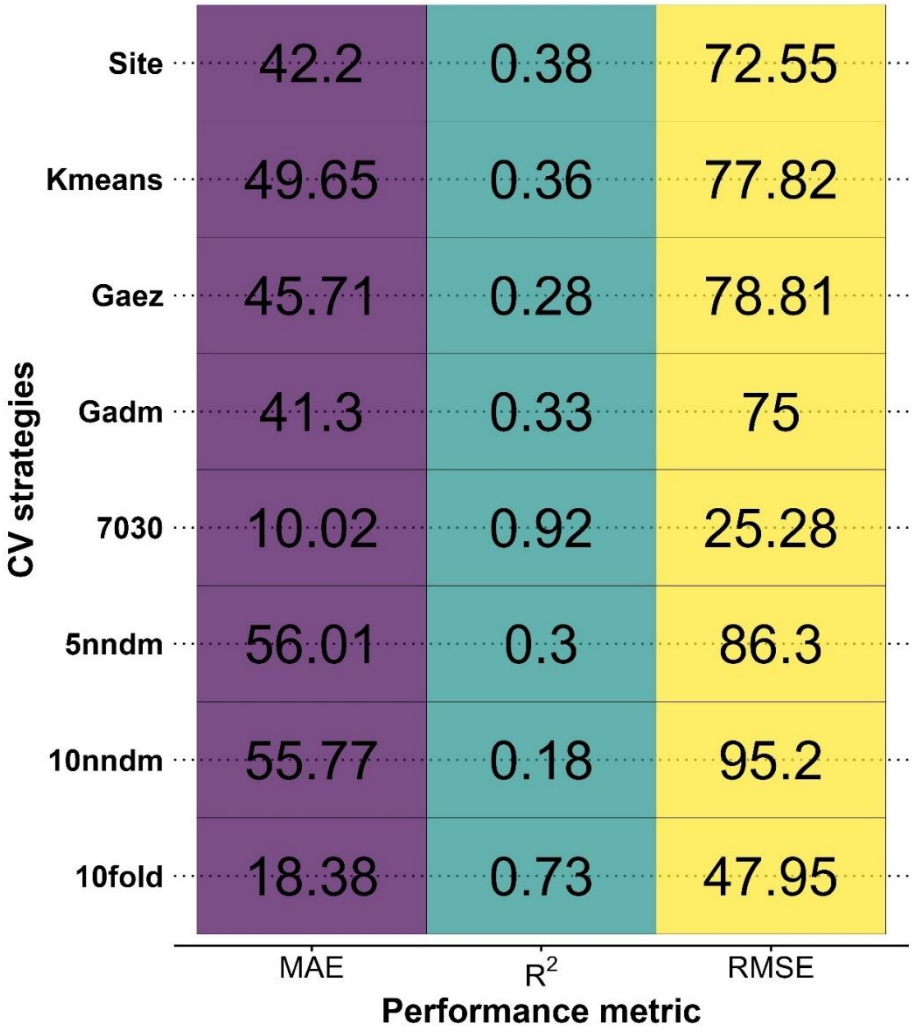

Figure S13. Performance metrics for each one of the hyper-tuned random forests models according to cross-validation sampling strategies. RMSE is the root mean square error, R2 is the coefficient of determination and MAE is the mean absolute error. Note that these metrics are weighted averages according to the number of observations in the folds. The final model chosen was with spatial cross validation stratified by site with the following random forest models parameters: mtry – 30; splitrule – variance; number of trees – 500.

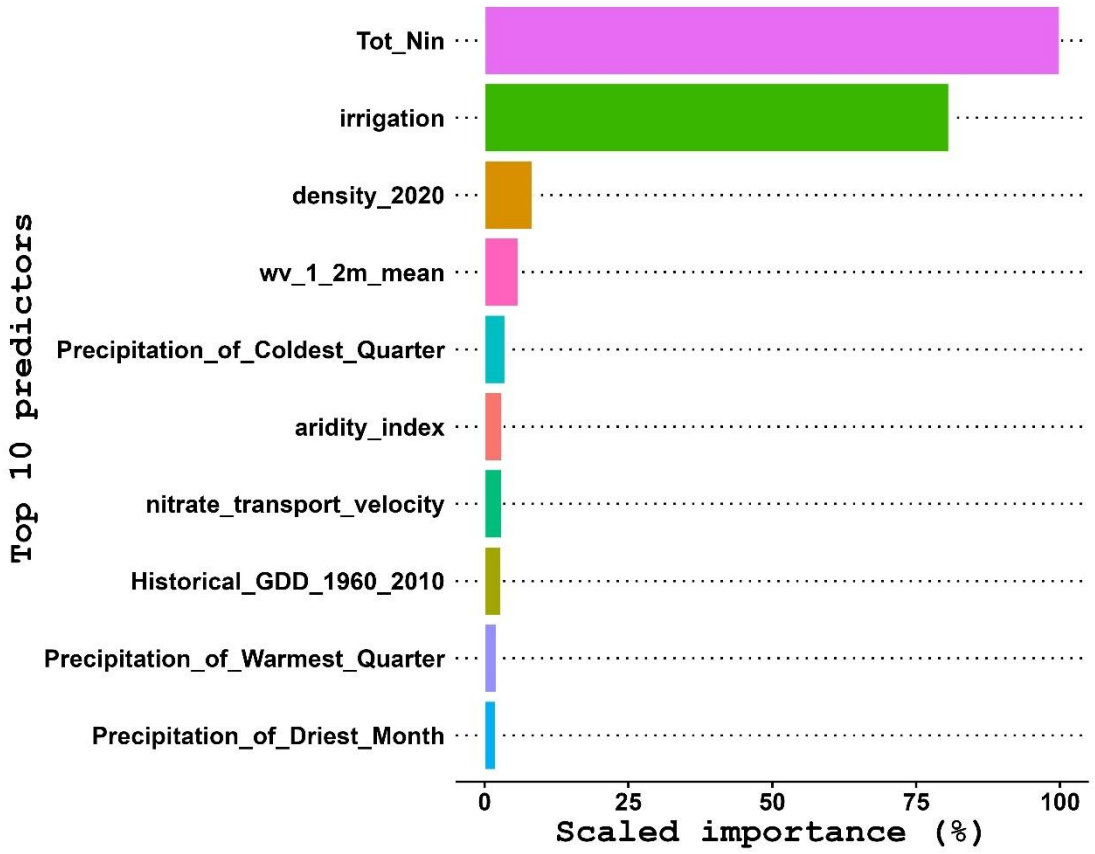

Figure S*14*. Variable importance of the random forest model.

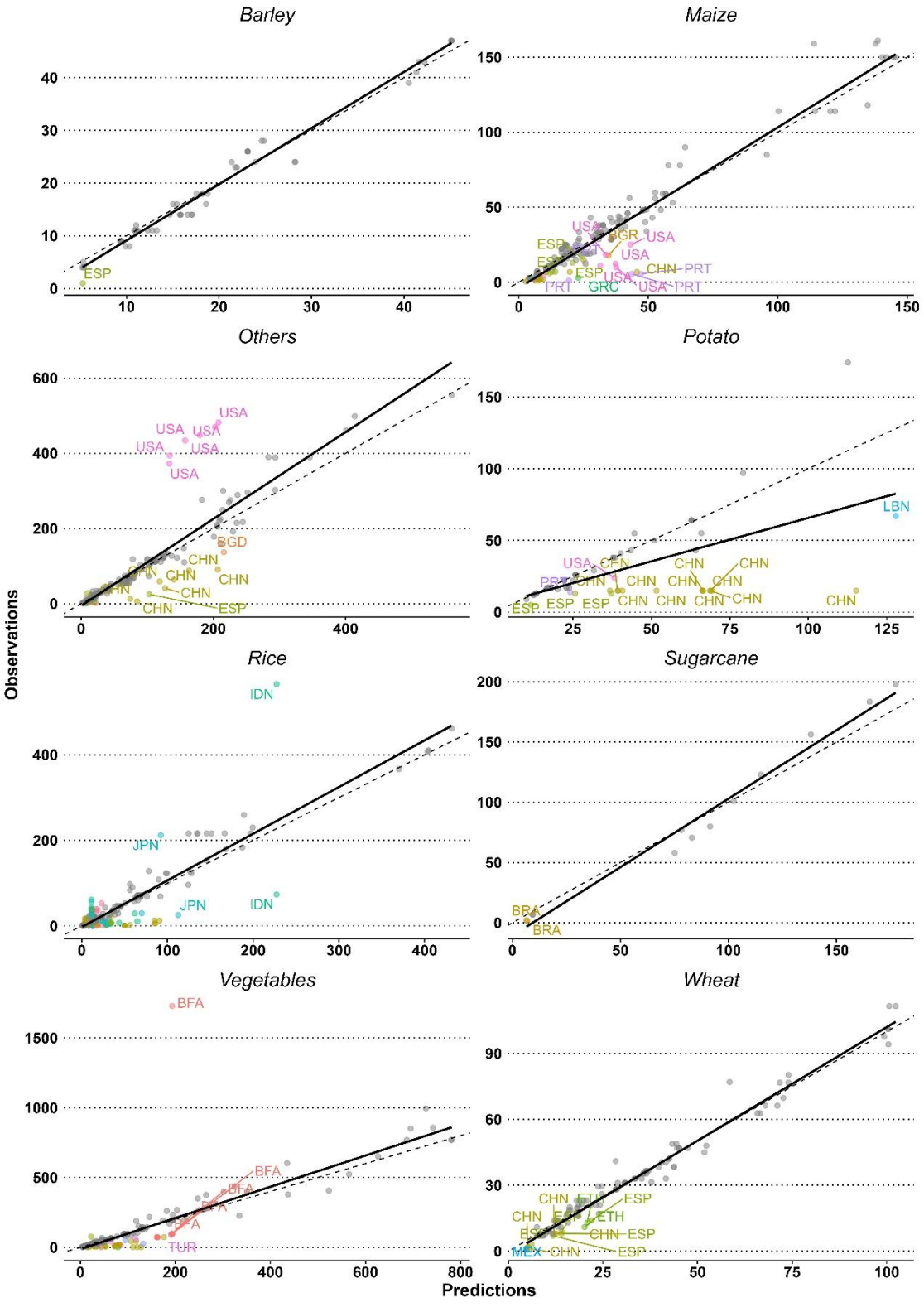

Figure S*15*. Correspondence between the predicted and observed N_{Irrig} for the whole observational dataset. Observations where the predictions exceed more than 50% are highlighted according to their country.

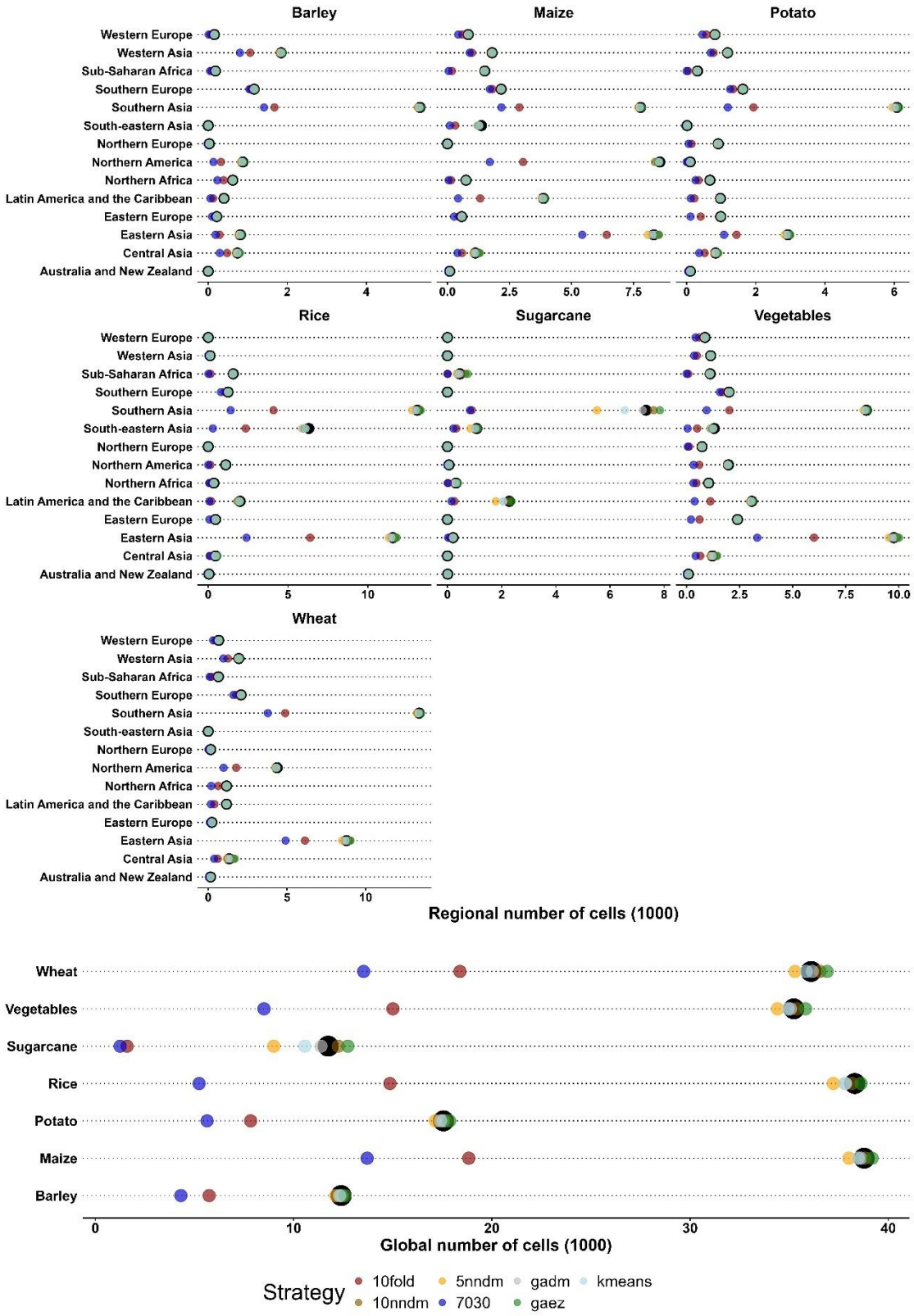

Figure S16. Regional (top) and global (bottom) sum of number of cells inside area of applicability per crop and sampling strategy. Black point represents the final strategy, a leave-one-out cross validation stratified by site.

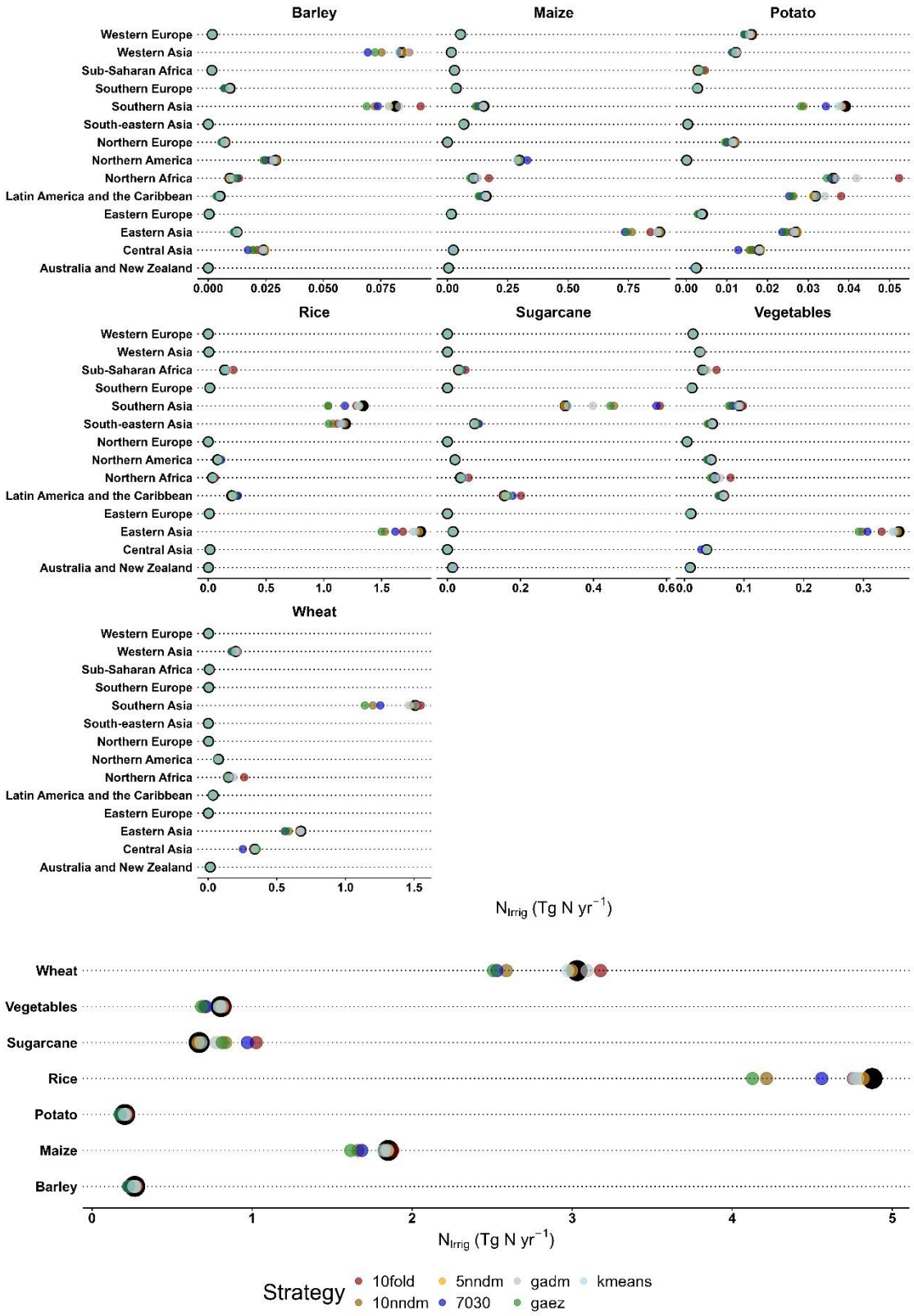

Figure S17. Regional (top) and global (bottom) sum of N_{Irrig} per crop and sampling strategy. Black point represents the final strategy, a leave-one-out cross validation stratified by site.

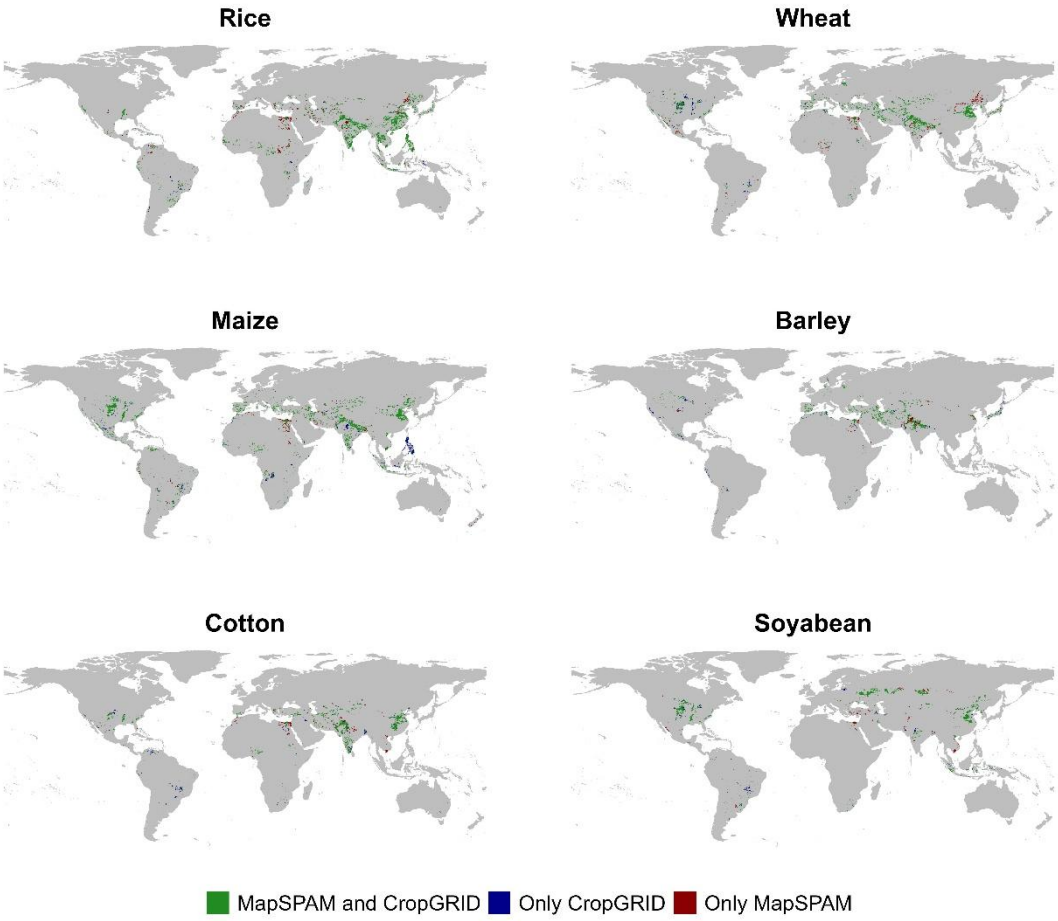

Figure S18. Comparison of MapSPAM 2020 (https://mapspam.info/) with CropGRID[29] for selected crops. Note that crop maps from CropGRID concern total harvested area (rainfed plus irrigated). Dark red areas may be "ghost" irrigated areas in MapSPAM since these should overlap with total harvested areas from CropGRID.

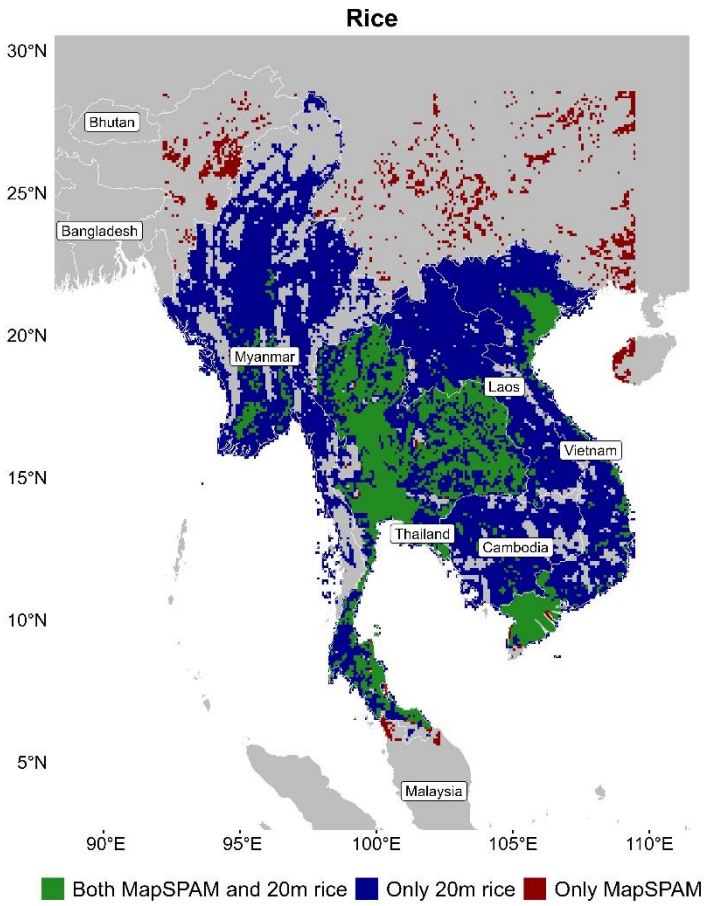

Figure S19. Comparison of MapSPAM 2020 (https://mapspam.info/) with 20m annual lowland rice area for mainland Southeast Asia for circa 2019[30]. Note that the annual 20m lowland rice area concerns total harvested area (rainfed plus irrigated) and was aggregated from 20m to 10km by summing 20m cells where rice is planted (set to 1). Dark red areas may be "ghost" irrigated areas in MapSPAM since these should overlap with total harvested areas.

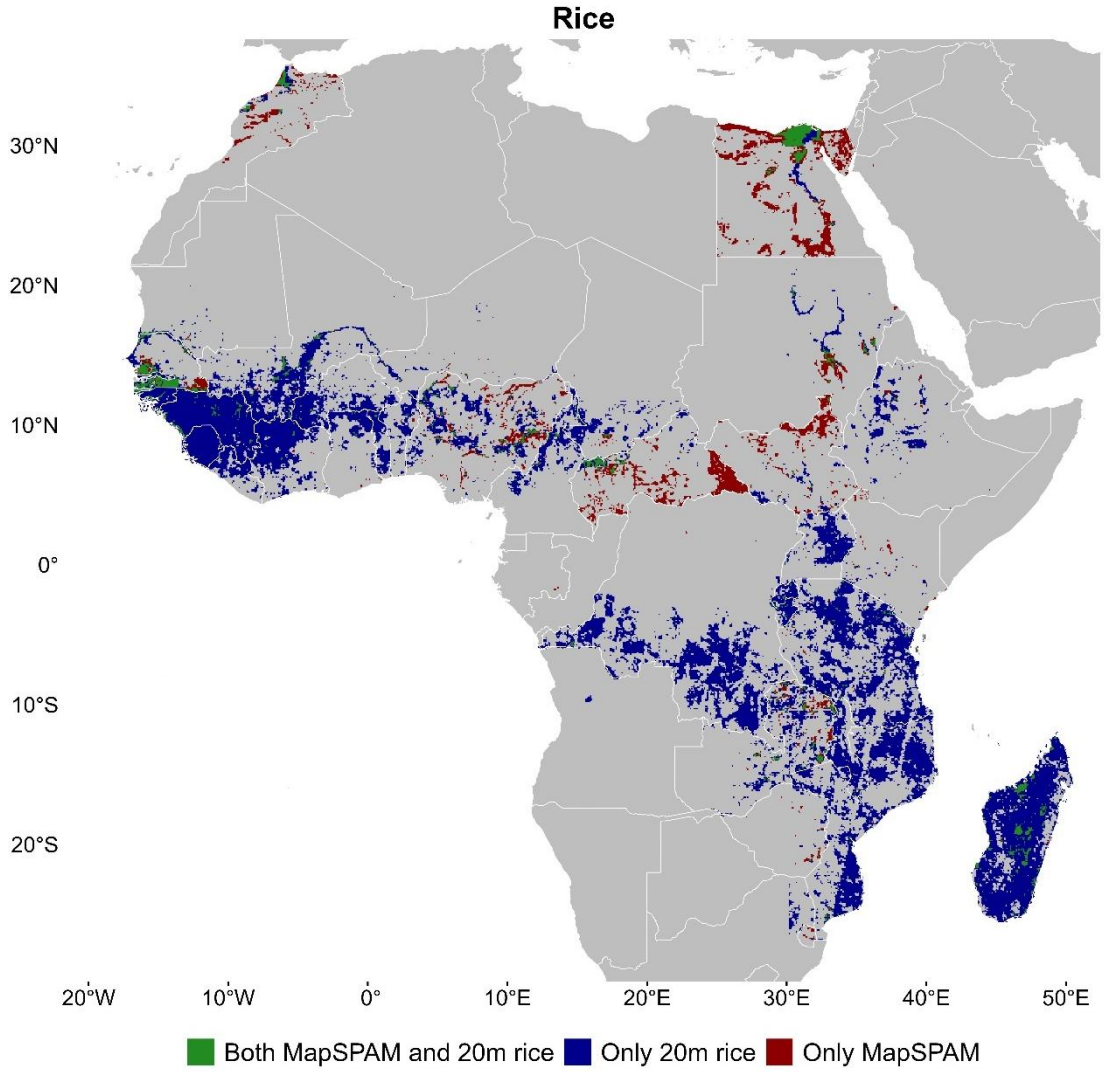

Figure S20. Comparison of MapSPAM 2020 (https://mapspam.info/) with 20m annual lowland rice area for Africa for 2023[31]. Note that the annual 20m lowland rice area concerns total harvested area (rainfed plus irrigated) and was aggregated from 20m to 10km by summing 20m cells where rice is planted (set to 1). Dark red areas may be "ghost" irrigated areas in MapSPAM since these should overlap with total harvested areas.

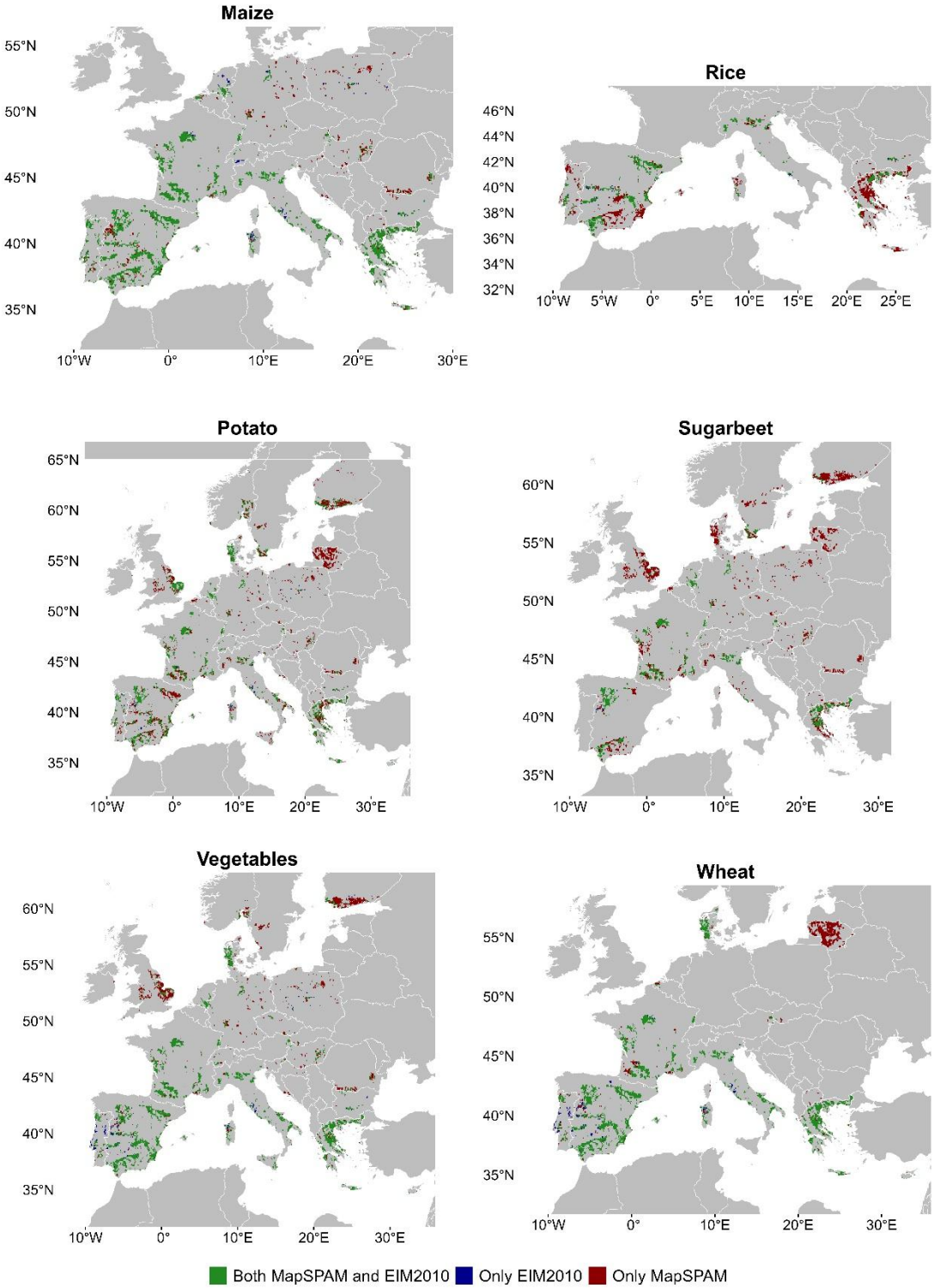

Figure S21. Comparison of MapSPAM 2020 (https://mapspam.info/) with European Irrigation Maps (EIM2010)[32] of different crops circa 2010. Dark red areas may be "ghost" irrigated areas in MapSPAM since these are not coherent with sub-national agricultural census from EIM2010.

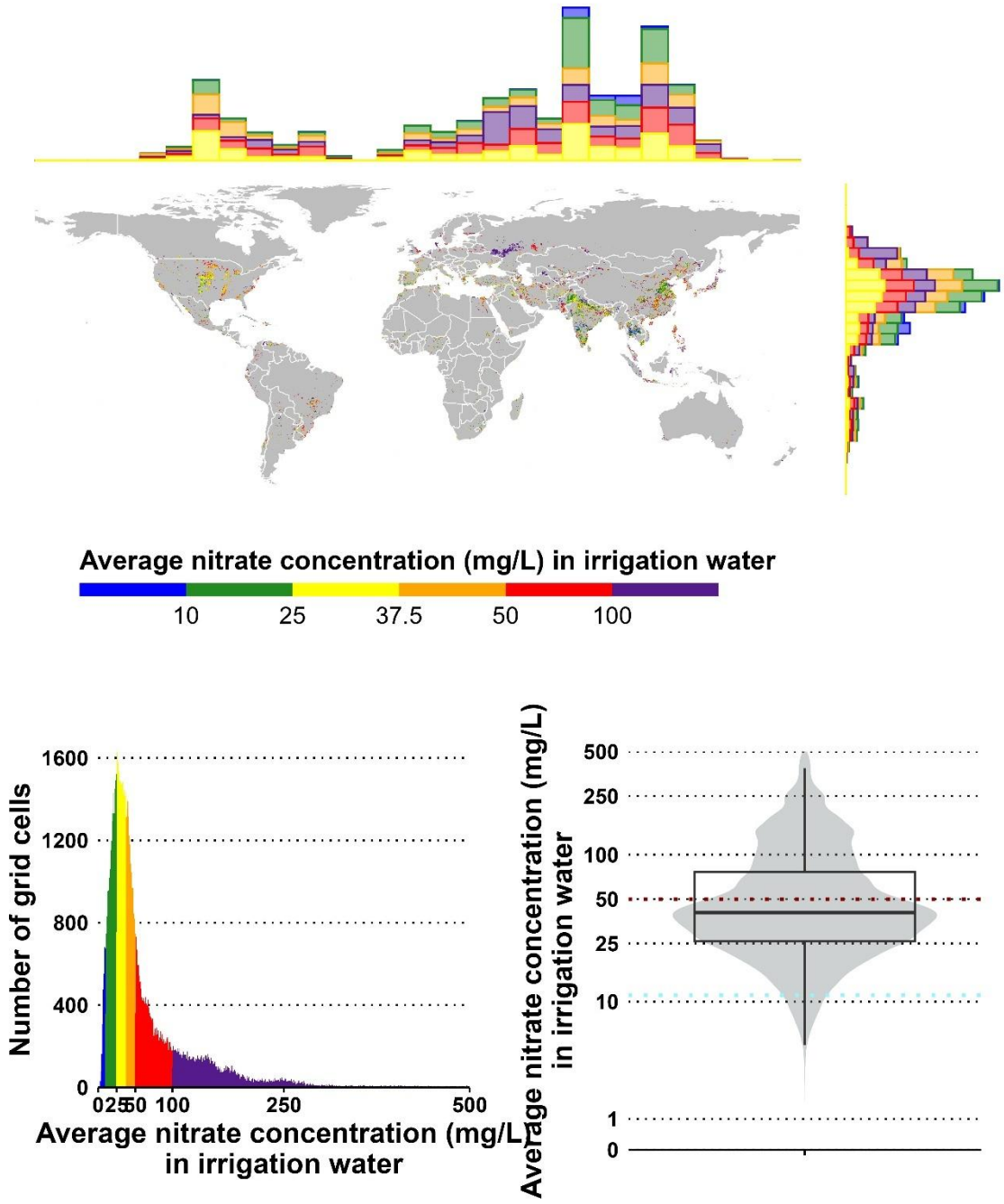

Figure S22. Derived averaged nitrate concentration in irrigation water sources, calculated as the ratio of the total N_{Irrig} and total volumes of irrigation water (top), as well as their distribution (bottom). The horizontal lines represent a typical environmental threshold for eutrophication in surface waters (2.5 mg L^{-1}) and the EU threshold for nitrate in drinking water (50 mg L^{-1}).

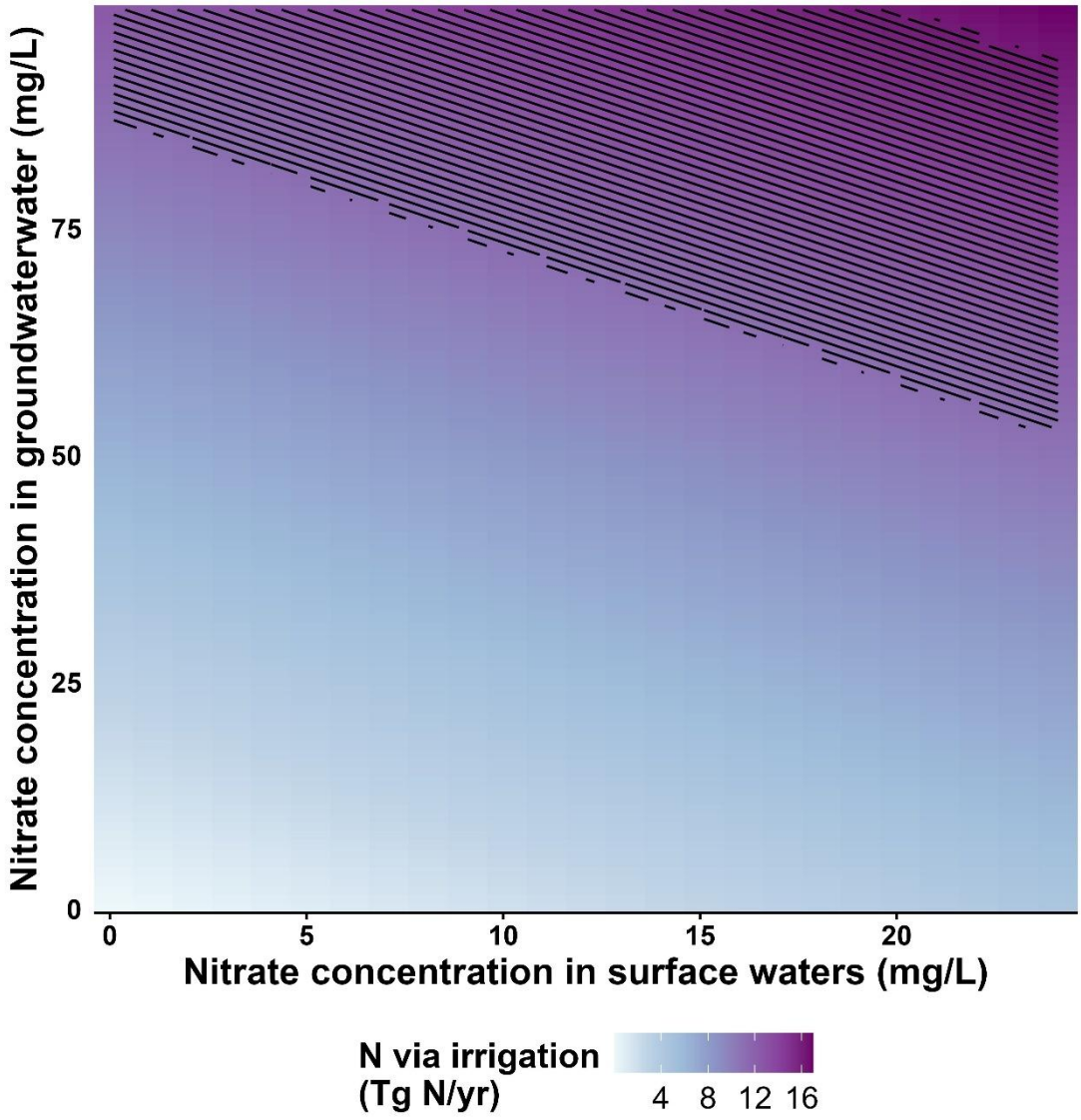

Figure S23. Factorial design of varying uniform nitrate concentrations in ground- and surface waters and their implications in the total global N_{Irrig} estimates. Contour lines represent ± 20% of our global estimate of 13.8 Tg N yr^{-1} as a proxy for possible variation.

References

1. Tian, H. *et al.* History of anthropogenic Nitrogen inputs (HaNi) to the terrestrial biosphere: a 5 arcmin resolution annual dataset from 1860 to 2019. *Earth System Science Data* **14**, 4551–4568 (2022).
2. Herridge, D. F., Giller, K. E., Jensen, E. S. & Peoples, M. B. Quantifying country-to-global scale nitrogen fixation for grain legumes II. Coefficients, templates and estimates for soybean, groundnut and pulses. *Plant Soil* **474**, 1–15 (2022).
3. Meyer, H., Ludwig, M., Milà, C., Linnenbrink, J. & Schumacher, F. The CAST package for training and assessment of spatial prediction models in R. Preprint at https://doi.org/10.48550/arXiv.2404.06978 (2024).
4. Linnenbrink, J., Milà, C., Ludwig, M. & Meyer, H. kNNDM CV: *k*-fold nearest-neighbour distance matching cross-validation for map accuracy estimation. *Geoscientific Model Development* **17**, 5897–5912 (2024).
5. Serra, J. *et al.* Assessing nitrate groundwater hotspots in Europe reveals an inadequate designation of Nitrate Vulnerable Zones. *Chemosphere* **355**, 141830 (2024).
6. Siebert, S. *et al.* Groundwater use for irrigation – a global inventory. *Hydrology and Earth System Sciences* **14**, 1863–1880 (2010).
7. Liu, X. *et al.* Chronic nitrogen legacy in the aquifers of China. *Commun Earth Environ* **6**, 58 (2025).
8. Serra, J. *et al.* Nitrogen inputs by irrigation is a missing link in the agricultural nitrogen cycle and related policies in Europe. *Science of The Total Environment* **889**, 164249 (2023).

9. Serra, J. *et al.* Is irrigation water an overlooked source of nitrogen in agriculture? *Agricultural Water Management* **278**, 108147 (2023).
10. Liu, J. *et al.* A high-resolution assessment on global nitrogen flows in cropland. *Proceedings of the National Academy of Sciences* **107**, 8035–8040 (2010).
11. Lesschen, J. P., Stoorvogel, J. J., Smaling, E. M. A., Heuvelink, G. B. M. & Veldkamp, A. A spatially explicit methodology to quantify soil nutrient balances and their uncertainties at the national level. *Nutr Cycl Agroecosyst* **78**, 111–131 (2007).
12. Flint, E. M., Ascott, M. J., Gooddy, D. C., Stahl, M. O. & Surridge, B. W. J. Water Supply Processes Are Responsible for Significant Nitrogen Fluxes Across the United States. *Global Biogeochemical Cycles* **36**, e2022GB007340 (2022).
13. Gu, B. *et al.* Cost-effective mitigation of nitrogen pollution from global croplands. *Nature* **613**, 77–84 (2023).
14. Yin, Y. *et al.* A steady-state N balance approach for sustainable smallholder farming. *Proceedings of the National Academy of Sciences* **118**, e2106576118 (2021).
15. Zheng, M. *et al.* Changes in nitrogen budget and potential risk to the environment over 20 years (1990–2010) in the agroecosystems of the Haihe Basin, China. *Journal of Environmental Sciences* **28**, 195–202 (2015).
16. He, W. *et al.* Estimating soil nitrogen balance at regional scale in China's croplands from 1984 to 2014. *Agricultural Systems* **167**, 125–135 (2018).

17. Wang, X. *et al.* Spatial variability of the nutrient balance and related NPSP risk analysis for agro-ecosystems in China in 2010. *Agriculture, Ecosystems & Environment* **193**, 42–52 (2014).
18. Smil, V. Nitrogen in crop production: An account of global flows. *Global Biogeochemical Cycles* **13**, 647–662 (1999).
19. klanmiko. The California Nitrogen Assessment | Sustainable Agriculture Research & Education Program. https://sarep.ucdavis.edu/are/nutrient/nitrogen/intro (2018).
20. Hayashi, K. *et al.* Nitrogen budgets in Japan from 2000 to 2015: Decreasing trend of nitrogen loss to the environment and the challenge to further reduce nitrogen waste. *Environmental Pollution* **286**, 117559 (2021).
21. Mialyk, O. *et al.* Water footprints and crop water use of 175 individual crops for 1990–2019 simulated with a global crop model. *Sci Data* **11**, 206 (2024).
22. Kummu, M., Kosonen, M. & Masoumzadeh Sayyar, S. Downscaled gridded global dataset for gross domestic product (GDP) per capita PPP over 1990–2022. *Sci Data* **12**, 178 (2025).
23. Global Patterns of Groundwater Table Depth | Science. https://www.science.org/doi/10.1126/science.1229881.
24. Richts, A., Struckmeier, W. F. & Zaepke, M. WHYMAP and the Groundwater Resources Map of the World 1:25,000,000. in *Sustaining Groundwater Resources* (ed. Jones, J. A. A.) 159–173 (Springer Netherlands, Dordrecht, 2011). doi:10.1007/978-90-481-3426-7_10.
25. Yang, C. *et al.* Nitrate transport velocity data in the global unsaturated zones. *Sci Data* **9**, 613 (2022).

26. Gleeson, T. GLobal HYdrogeology MaPS (GLHYMPS) of permeability and porosity. Borealis https://doi.org/10.5683/SP2/DLGXYO (2018).
27. Kummu, M., Moel, H. de, Ward, P. J. & Varis, O. How Close Do We Live to Water? A Global Analysis of Population Distance to Freshwater Bodies. *PLOS ONE* **6**, e20578 (2011).
28. Zomer, R. J., Xu, J. & Trabucco, A. Version 3 of the Global Aridity Index and Potential Evapotranspiration Database. *Sci Data* **9**, 409 (2022).
29. Tang, F. H. M. *et al.* CROPGRIDS: a global geo-referenced dataset of 173 crops. *Sci Data* **11**, 413 (2024).
30. Sun, C. *et al.* Twenty-meter annual paddy rice area map for mainland Southeast Asia using Sentinel-1 synthetic-aperture-radar data. *Earth System Science Data* **15**, 1501–1520 (2023).
31. ESSDD - 20 m Africa Rice Distribution Map of 2023. https://essd.copernicus.org/preprints/essd-2024-402/.
32. Zajac, Z. *et al.* Estimation of spatial distribution of irrigated crop areas in Europe for large-scale modelling applications. *Agricultural Water Management* **266**, 107527 (2022).